

Wave-blocking Efficiency of a Horizontal Porous Flexible Membrane

IL-HYOUNG CHO*

*Department of Marine Industrial Engineering, Cheju National University, Jeju, Korea

KEY WORDS : Horizontal Porous Flexible Membrane, Linear Hydro-elastic Theory, Eigenfunction Expansion Method, Transmission Coefficient, Reflection Coefficient, Energy Loss Coefficient

ABSTRACT : 본 논문에서는 투과성 유연막이 수면 밑 일정한 깊이에서 수평으로 잠겨있을 때 투과성 유연막에 의한 파랑 제어 성능을 살펴보았다. 해석 방법으로는 유체문제는 고유함수전개법 (Eigenfunction expansion method)을 사용하였고, 유연막과 파랑의 상호작용문제는 Neumann이 제시한 유탄성 이론 (hydro-elastic theory)을 채택하였다. 막의 투과성 효과를 고려하기 위하여 수평 막에서의 수직속도는 수평막 상하의 압력차에 선형적으로 비례하며 그들 사이에는 위상차가 없다고 가정한 Darcy 법칙을 사용하였다. 투과성 수평막의 설계변수 (초기장력, 길이, 잠긴 깊이, 공극율)와 입사파의 주파수를 바꿔가면서 반사율과 투과율 그리고 에너지 손실율을 살펴보았다.

1. Introduction

Various floating breakwaters have been proposed for the protection of small marinas and recreational harbors. However, most floating wave barriers are known to be ineffective, unless its size is comparable to 1/4 to 1/2 wave length, which results in high construction cost. During the past decade, there has been a gradual increase of interest in the use of flexible membrane as an effective, inexpensive wave barrier. In particular, the membrane is light and rapidly deployable; thus, it may be an ideal candidate as a portable temporary breakwater.

The performance of a vertical-screen membrane breakwater was investigated by Thomson et al. (1992), Aoki et al. (1994), Kim and Kee (1996), and Cho et al. (1997). Using the linear wave theory and membrane-motion equation, Kim and Kee (1996) and Cho et al. (1997) showed that almost complete reflection was possible, despite appreciable sinusoidal motions of the membrane, which tend to generate only exponentially-decaying, local (evanescent) waves in the lee side. The theory was compared, favorably, with 2-D tank experiments (Kim and Kee, 1996).

Some major problems associated with the use of flexible vertical screen are the expected large wave loading and possible blockage of currents or surface vessels. In view of this, the feasibility of an alternative horizontal membrane, as a wave barrier, was investigated by Cho and Kim (1998).

Since the horizontal membrane does not directly block incoming

waves, the diffracted and radiated waves, including various elastic modes, have to be properly tuned in order to be an effective wave barrier. It is shown in Cho and Kim (1998) that the overall wave-blocking efficiency can be greatly improved by allowing membrane flexibility compared to rigid plates.

The performance of a horizontal flexible membrane can be further enhanced by adding a proper porosity to the membrane surface. The resulting wave loads can also be significantly reduced by membrane porosity. Isaacson (1998), for example, developed a numerical model to describe the wave interaction with a permeable thin vertical barrier, and found that the porous effect reduces not only the wave amplitude, but also the hydrodynamic force on the permeable barrier. Yu and Chwang (1994) applied the boundary element method to investigate the reflection and transmission of surface waves by a horizontally submerged porous plate. Wu et al. (1998) investigated wave reflection using a vertical wall with a submerged horizontal porous plate. It was found that, with proper porosity the plate can significantly reduce not only the wave height above the plate, but also the reflection coefficient. Recently, Cho and Kim (2000) solved the interaction problem of incident waves with a horizontal porous flexible membrane using the eigenfunction expansion method and the boundary element method, under the assumption of linear hydro-elastic theory.

In this paper, analytical solutions are obtained by an eigenfunction expansion approach to investigate the effect of membrane porosity on the wave-blocking efficiency of a horizontal flexible membrane.

It is assumed that the membrane is made of material with

제1저자 조일형 연락처: 제주도 제주시 아라동 1번지

064-754-3482 cho0904@cheju.ac.kr

very fine pores, so that the normal velocity of the fluid passing through the porous membrane is linearly proportional to the pressure difference between the two sides of the membrane. The same porosity model was also used by Chwang and Yu (1994), Cho and Kim (2000), and Wu et al. (1998). It is found that the enhancement of wave-blocking efficiency by viscous dissipation through pores is more pronounced when the porous membrane is located closer to the free surface.

2. Mathematical Formulation

We explore the interaction of a horizontal porous membrane wave barrier with monochromatic incident waves. Cartesian axes are chosen with the x -axis along the mean free surface and the y -axis pointing vertically upwards. The water depth is denoted by h and the submergence depth of the membrane by d . It is assumed that both ends of the membrane are fixed at $x = \pm a$, and a uniform tension T is applied on the membrane in the x direction (see Fig.1).

It is also assumed that the fluid is ideal, except for the pore region, and the wave and membrane motions are small, so that linear potential theory can be used. The fluid particle velocity can then be described by the gradient of a velocity potential $\Phi(x, y, t)$.

Assuming harmonic motion of frequency ω , the velocity potential can be written as $\Phi(x, y, t) = \text{Re}\{\phi(x, y)e^{-i\omega t}\}$.

The wave number k_1 satisfies the dispersion relation, $\omega^2 = gk_1 \tanh k_1 h$. Similarly, the vertical displacement of the membrane can be written as:

$$\Xi(x, t) = \text{Re}\{\xi(x)e^{-i\omega t}\} \quad (1)$$

where $\xi(x)$ is the complex displacement of the membrane.

The velocity potential ϕ satisfies the Laplace equation

$$\frac{\partial^2 \phi}{\partial x^2} + \frac{\partial^2 \phi}{\partial y^2} = 0 \text{ in the fluid} \quad (2)$$

with the following boundary conditions:

$$\partial \phi / \partial y - \nu \phi = 0 \quad (\nu = \omega^2 / g) \text{ on } y = 0 \quad (3)$$

$$\frac{\partial \phi}{\partial y} = 0 \text{ on } y = -h \quad (4)$$

$$\lim_{|x| \rightarrow \infty} \left(\frac{\partial \phi}{\partial x} \pm ik_1 \phi \right) = 0 \text{ at far field} \quad (5)$$

$$\frac{\partial \phi}{\partial y} \Big|_{y=-d+0} = -i\omega \xi + i\sigma(\phi|_{y=-d-0} - \phi|_{y=-d+0}) \quad (6)$$

on $-a \leq x \leq a$

where σ is the real positive porous-effect parameter ($= \frac{\rho b_o \omega}{\mu}$) with b_o =porosity coefficient, ρ =fluid density, and μ =dynamic viscosity of the fluid. It is assumed in (6) that the membrane is made of material with very fine pores, so that the normal velocity of the fluid passing through the porous membrane is linearly proportional to the pressure difference between the two sides of the membrane (Chwang and Yu, 1994; Wu et al., 1998).

The limiting case $b_o \rightarrow 0$ corresponds to the impermeable membrane and $b_o \rightarrow \infty$ means that the membrane is infinitely porous equivalent to no obstruction in the fluid domain.

On the membrane surface, the following dynamic condition has to be satisfied (Cho and Kim, 1998):

$$-\frac{d^2 \xi}{dx^2} + \lambda^2 \xi = -\frac{i\rho\omega}{T} [\phi^{(2)}(x-d-0) - \phi^{(2)}(x, 0-d+0)] \quad (7)$$

in which $\lambda = \omega \sqrt{m/T}$ with T and m being the membrane tension and mass per unit length, respectively. Here, it is assumed that the initial tension is large, so that the effect of dynamic tension can be neglected. The complex displacement of the membrane can be expanded in terms of a set of natural modes of the membrane:

$$\xi(x) = \sum_{l=0}^{\infty} \zeta_l f_l(x) \quad (8)$$

where ζ_l is the unknown complex modal amplitude, corresponding to the l -th mode. The modal functions and eigenvalues of the membrane satisfying the membrane equation (7) and the end condition are given by (e.g. Cho and Kim, 1998)

$$f_l(x) = \begin{cases} f_l^S(x) = \cos \frac{\lambda_l^S x}{a}, & \lambda_l^S = \frac{[2(l-1)+1]\pi}{2} \\ f_l^A(x) = \sin \frac{\lambda_l^A x}{a}, & \lambda_l^A = l\pi \quad (l=1, 2, 3, \dots) \end{cases} \quad (9)$$

where the superscripts S and A denote symmetric and asymmetric modes about $x=0$, respectively. The modal functions given in equation (9) are orthogonal to each other in the interval $[-a, a]$:

$$\int_{-a}^a f_i(x) f_j(x) dx = \begin{cases} a & i=j \\ 0 & i \neq j \end{cases} \quad (10)$$

Including all the flexible membrane modes, the complex potential $\phi(x, y)$ can be expressed in the form:

$$\phi(x, y) = \phi_D(x, y) + \sum_{l=0}^{\infty} \zeta_l \phi_{lR}(x, y), \quad (11)$$

$$\phi_D(x, y) = \phi_I(x, y) + \phi_S(x, y)$$

where ϕ_D is the diffraction potential and ϕ_S, ϕ_{IR} denote the scattering and radiation potential, respectively. The incident wave potential ϕ_I with wave amplitude $A=1$ is given by :

$$\phi_I(x, y) = -\frac{ig}{\omega} \frac{\cosh k_1(y+h)}{\cosh k_1 h} e^{ik_1 x} \quad (12)$$

3. Analytic Solutions

The fluid domain is divided into two regions, as shown in Fig.1. Region (I) is defined by $x \leq -a, -h < y < 0$, and region (II) by $|x| \leq a, -h < y < 0$.

The diffraction potential satisfies the governing equation (2), boundary conditions (3)-(5), and (6) with $\xi=0$. In the following, the symmetry of the fluid and membrane is used by splitting ϕ_D into symmetric and asymmetric parts.

$$\phi_D(x, y) = \phi_D^S(x, y) + \phi_D^A(x, y) \quad (13a)$$

where

$$\begin{aligned} \phi_D^S(-x, y) &= \phi_D^S(x, y), \quad \frac{\partial \phi_D^S}{\partial x} = 0 \quad \text{on } x=0 \\ \phi_D^A(-x, y) &= -\phi_D^A(x, y), \quad \phi_D^A = 0 \quad \text{on } x=0 \end{aligned} \quad (13b)$$

The symmetric diffraction potential in each fluid region can be written as follows :

$$\phi_D^{S(1)} = -\frac{ig}{\omega} \left\{ \frac{1}{2} e^{-k_{10}x} f_{10}(y) + \sum_{n=0}^{\infty} a_n^S e^{k_{1n}(x+a)} f_{1n}(y) \right\} \quad (14)$$

$$\phi_D^{S(2)} = -\frac{ig}{\omega} \sum_{n=0}^{\infty} b_n^S \cos k_{2n}x f_{2n}(y) \quad (15)$$

where $k_{10} = -ik_1$, and the eigenfunctions $f_{1n}(y)$ are given by

$$f_{1n}(y) = \begin{cases} \frac{\cosh k_1(y+h)}{\cosh k_1 h} & n=0 \\ \frac{\cos k_{1n}(y+h)}{\cos k_{1n} h} & n \geq 1 \end{cases} \quad (16)$$

The eigenvalues are the solutions of the following equations:

$$\begin{cases} k_1 \tanh k_1 h = \frac{\omega^2}{g} & n=0 \\ k_{1n} \tan k_{1n} h = -\frac{\omega^2}{g} & n \geq 1 \end{cases} \quad (17)$$

The eigenfunctions $f_{2n}(y)$ and eigenvalues k_{2n} satisfy the following eigenvalue-problem :

$$\frac{d^2 f}{dy^2} - \chi^2 f = 0$$

$$\frac{df}{dy} - \nu f = 0 \quad \text{on } y=0$$

$$\frac{df}{dy} \Big|_{y=-d+0} = \frac{df}{dy} \Big|_{y=-d-0} = i\sigma (f_{y=-d-0} - f_{y=-d+0})$$

$$\frac{df}{dy} = 0 \quad \text{on } y=-h$$

(18)

for the upper complex plane of χ and $0 < \sigma < \infty$. The complex eigenvalues k_{2n} are the roots of the following equation :

$$\begin{aligned} &x \sinh x(h-d)(\nu \cosh xd - x \sinh xd) \\ &- i\sigma(\nu \cosh xh - x \sinh xh) = 0 \end{aligned} \quad (19)$$

There exist an infinite number of discrete complex roots $\chi = \chi_1 + i\chi_2$. The real and imaginary parts of the left-hand side of (19) must be zero. The nonlinear equation (19) is solved using a Newton-Raphson iteration method. The initial values were determined from the case without porosity. The resulting eigenfunctions $f_{2n}(y)$ are

$$\begin{aligned} f_{2n}(y) &= \begin{cases} \sinh k_{2n}(h-d)(k_{2n} \cosh k_{2n}y + \nu \sinh k_{2n}y) - d \leq y \leq 0 \\ (\nu \cosh k_{2n}d - k_{2n} \sinh k_{2n}d) \cosh k_{2n}(y+h) - h \leq y \leq -d \end{cases} \end{aligned} \quad (20)$$

By using (20), it can be shown that the eigenfunctions are orthogonal to each another. If $\sigma \rightarrow 0$, the solutions of the above eigenfunction problem become identical to those of impermeable membrane (Cho and Kim, 1998). As $\sigma \rightarrow \infty$, the porous membrane becomes completely permeable, and the incident wave propagates without any obstruction.

The unknown coefficients $a_n^S, b_n^S (n=0, 1, 2, \dots)$ in (14) and (15) are determined by invoking the continuity of potentials and horizontal velocities on $x=-a$. The final matrix equation can then be obtained as follows:

$$\begin{aligned} a_0^S + \sum_{k=0}^{\infty} \frac{F_{0k}^S}{k_{10}N_0^{(1)}} a_k^S &= \frac{1}{2} e^{k_{10}a} \left(1 - \frac{F_{00}^S}{k_{10}N_0^{(1)}} \right) \quad m=0, \\ a_m^S + \sum_{k=0}^{\infty} \frac{F_{mk}^S}{k_{1m}N_m^{(1)}} a_k^S &= -\frac{1}{2} e^{k_{10}a} \frac{F_{m0}^S}{k_{1m}N_m^{(1)}} \quad m=1, 2, 3, \dots \end{aligned} \quad (21)$$

where

$$\int_{-h}^0 f_{1n}(y) f_{1m}(y) dy = \begin{cases} N_m^{(1)} & m=n \\ 0 & m \neq n \end{cases} \quad (22)$$

$$F_{mk}^S = -\sum_{n=0}^{\infty} \frac{k_{2n} \tan k_{2n} a C_{nm} C_{nk}}{N_n^{(2)}} \quad (23)$$

$$C_{mn} = \int_{-h}^0 f_{1n}(y) f_{2m}(y) dy \quad (24)$$

$$\int_{-h}^0 f_{2n}(y) f_{2m}(y) dy = \begin{cases} N_n^{(2)} & m=n \\ 0 & m \neq n \end{cases}$$

By solving the above algebraic equation, the unknown constants a_n^S in region (I) can be determined. The other unknown constants b_n^S in region (II) can be determined in a similar manner:

$$b_n^S = \frac{\frac{1}{2} e^{k_{10}a} C_{n0} + \sum_{k=0}^{\infty} a_k^S C_{nk}}{\cos k_{2n}a N_n^{(2)}} \quad n \geq 0, \quad (25)$$

Similarly, the asymmetric diffraction potential in each fluid region can be written as

$$\phi_D^{A(1)} = -\frac{ig}{\omega} \left\{ \frac{1}{2} e^{-k_{10}x} f_{10}(y) + \sum_{n=0}^{\infty} a_n^A e^{k_{1n}(x+a)} f_{1n}(y) \right\} \quad (26)$$

$$\phi_D^{A(2)} = -\frac{ig}{\omega} \sum_{n=0}^{\infty} b_n^A \sin k_{2n}x f_{2n}(y) \quad (27)$$

The unknown coefficients $a_n^A, b_n^A (n=0, 1, 2, \dots)$ are determined after applying the matching conditions on :

$$a_0^A + \sum_{k=0}^{\infty} \frac{F_{0k}^A}{k_{10}N_0^{(1)}} a_k^A = -\frac{1}{2} e^{k_{10}a} \left(\frac{F_{00}^A}{k_{10}N_0^{(1)}} - 1 \right) \quad m=0,$$

$$a_m^A + \sum_{k=0}^{\infty} \frac{F_{mk}^A}{k_{1m}N_m^{(1)}} a_k^A = -\frac{1}{2} e^{k_{10}a} \frac{F_{m0}^A}{k_{1m}N_m^{(1)}} \quad m=1, 2, 3, \dots \quad (28)$$

where

$$F_{mk}^A = \sum_{n=0}^{\infty} \frac{k_{2n} \cot k_{2n}a C_{nm} C_{nk}}{N_n^{(2)}}. \quad (29)$$

The other unknown constants in region (II) can be obtained from

$$b_n^A = -\frac{\frac{1}{2} e^{k_{10}a} C_{n0} + \sum_{k=0}^{\infty} a_k^A C_{nk}}{\sin k_{2n}a N_n^{(2)}} \quad n \geq 0, \quad (30)$$

On the other hand, the radiation potential satisfies the following condition on the porous membrane:

$$\frac{\partial \phi_{IR}}{\partial y} \Big|_{y=-d \pm 0} = -i\omega f(x) + i\sigma(\phi_{IR} \Big|_{y=-d-0} - \phi_{IR} \Big|_{y=-d+0}) \quad (31)$$

Like the diffraction problem, the radiation potentials can be represented by the sum of homogeneous and particular solutions. The symmetric radiation potentials in each region can be written as follows:

$$\phi_{IR}^{S(1)} = -\frac{ig}{\omega} \sum_{n=0}^{\infty} a_{ln}^S e^{k_{1n}(x+a)} f_{1n}(y) \quad (32)$$

$$\phi_{IR}^{S(2)} = -\frac{ig}{\omega} \left\{ \sum_{n=0}^{\infty} b_{ln}^S \cos k_{2n}x f_{2n}(y) + \frac{i\omega}{g} \Psi_{IR}^{S(2)}(x, y) \right\} \quad (33)$$

Similarly, the asymmetric radiation potentials in each region are given in the form:

$$\phi_{IR}^{A(1)} = -\frac{ig}{\omega} \sum_{n=0}^{\infty} a_{ln}^A e^{k_{1n}(x+a)} f_{1n}(y) \quad (34)$$

$$\phi_{IR}^{A(2)} = -\frac{ig}{\omega} \left\{ \sum_{n=0}^{\infty} b_{ln}^A \sin k_{2n}x f_{2n}(y) + \frac{i\omega}{g} \Psi_{IR}^{A(2)}(x, y) \right\} \quad (35)$$

The particular solutions $\Psi_{IR}^{S(2)}, \Psi_{IR}^{A(2)}$ in region (II) satisfying the inhomogeneous membrane boundary condition are given by Cho and Kim(2000).

Finally, the algebraic equation for the unknown constants in region (I) can be derived after applying the matching conditions on $x = -a$ as follows:

$$a_{lm}^{S,A} + \sum_{k=0}^{\infty} \frac{F_{mk}^{S,A}}{k_{1m}N_m^{(1)}} a_{lk}^{S,A} = \frac{X_{ml}^{S,A}}{k_{1m}N_m^{(1)}} \quad m=0, 1, 2, \dots \quad (36)$$

where

$$X_{ml}^S = \frac{i\omega}{g} \int_{-h}^0 \frac{\partial \Psi_{IR}^{S(2)}(-a, y)}{\partial x} f_{1m}(y) dy \quad (37)$$

$$X_{ml}^A = \frac{i\omega}{g} \int_{-h}^0 \frac{\partial \Psi_{IR}^{A(2)}(-a, y)}{\partial x} f_{1m}(y) dy$$

The other unknown b_{ln}^S and b_{ln}^A coefficients can be determined from

$$b_{ln}^S = \frac{\sum_{k=0}^{\infty} a_{lk}^S C_{nk} - \frac{i\omega}{g} \int_{-h}^0 \Psi_{IR}^{S(2)}(-a, y) f_{2n}(y) dy}{\cos k_{2n}a N_n^{(2)}} \quad n \geq 0$$

$$b_{ln}^A = \frac{-\sum_{k=0}^{\infty} a_{lk}^A C_{nk} + \frac{i\omega}{g} \int_{-h}^0 \Psi_{IR}^{A(2)}(-a, y) f_{2n}(y) dy}{\sin k_{2n}a N_n^{(2)}} \quad n \geq 0 \quad (38)$$

Substituting $\phi(x, y) = \phi_D(x, y) + \sum_{j=1}^{\infty} \xi_j \phi_{IR}(x, y)$

$\xi(x) = \sum_{j=1}^{\infty} \xi_j f_j(x)$ into (7) yields

$$\sum_{j=1}^{\infty} \xi_j \left\{ -T \frac{d^2 f_j(x)}{dx^2} - m\omega^2 f_j(x) - p_{jR}(x) \right\} = p_D(x) \quad (39)$$

where

$$p_{jR}(x) = i\rho\omega \left[\phi_{jR}^{(2)}(x, -d-0) - \phi_{jR}^{(2)}(x, -d+0) \right] \quad (40)$$

$$p_D(x) = i\rho\omega \left[\phi_D^{(2)}(x, -d-0) - \phi_D^{(2)}(x, -d+0) \right]$$

Multiplying the above equation by $f_i(x)$ and integrating over the membrane, we obtain

$$\sum_{j=1}^{\infty} \{K_{ij} - \omega^2(M_{ij} + \widehat{a}_{ij}) - i\omega \widehat{b}_{ij}\} \zeta_j = F_i, \quad i=1, 2, \dots \quad (41)$$

where

$$\begin{aligned} K_{ij} &= - \int_{-a}^a T \frac{d^2 f_j(x)}{dx^2} f_i(x) dx \\ M_{ij} &= \int_{-a}^a m f_j(x) f_i(x) dx \\ \widehat{a}_{ij} &= \operatorname{Re} \left\{ \frac{1}{\omega^2} \int_{-a}^a p_{jR}(x) f_i(x) dx \right\} \\ \widehat{b}_{ij} &= \operatorname{Im} \left\{ \frac{1}{\omega} \int_{-a}^a p_{jR}(x) f_i(x) dx \right\} \\ F_i &= \int_{-a}^a p_D(x) f_i(x) dx \end{aligned} \quad (42)$$

The symbols K_{ij} , M_{ij} and F_i represent the generalized (modal) stiffness matrix, mass matrix, and force vector, respectively, and \widehat{a}_{ij} and \widehat{b}_{ij} are the generalized added-mass and radiation-damping matrix. Truncating the series of (41) at the appropriate term M , we can solve for the unknown complex amplitudes ζ_j corresponding to each mode (Newman, 1994).

Finally, the reflection and transmission coefficients can be determined from

$$\begin{aligned} R_f &= | [a_0^S + a_0^A] + \sum_{j=1}^{\infty} \zeta_j (a_{jR}^S + a_{jR}^A) | e^{k_{10} a_1}, \\ T_r &= | [a_0^S - a_0^A] + \sum_{j=1}^{\infty} \zeta_j (a_{jR}^S - a_{jR}^A) | e^{k_{10} a_1}, \end{aligned} \quad (43)$$

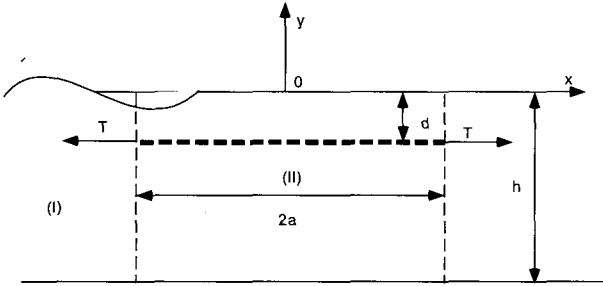


Fig. 1 Definition sketch for horizontal porous membrane

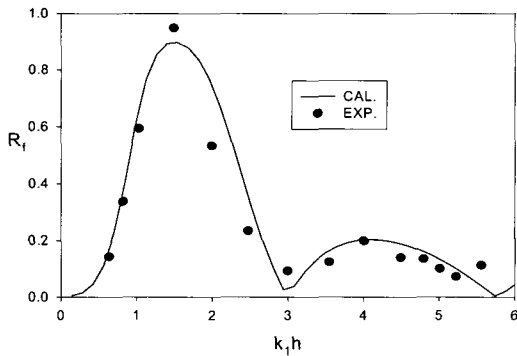


Fig. 2 Comparison between analytic and experimental results ($2a/h = 1.1$, $d/h = 0.182$)

4. Results and Discussions

In order to validate the analytic results developed, the analytic results for impermeable horizontal plate ($b \rightarrow 0, T \rightarrow \infty$) are compared with the experimental results conducted in the 2D wave tank. The model is made of a thin steel plate. The length and submergence depth of the plate are 60cm and 10.12cm, respectively. The water depth is fixed at 55cm. The measured reflection coefficients generally follow the trend of computed curves within the entire range of frequencies.

Reflection and transmission coefficients for impermeable horizontal plates with various b are shown in Fig.3. The porosity parameter b used in the figures is defined as

follows: $b = \frac{2\pi\sigma}{k_1} = \frac{2\pi\rho\omega b_0}{k_1\mu}$, where a large b represents

highly porous membrane and $b=0$ means that the membrane is impermeable. Both reflection and transmission curves with $b=5.0$ have low values within the entire range of frequencies. The rate of R_f decrease is larger when $1 < k_1 h < 3$; the transmission coefficient show the large rate of decrease in the high frequencies region.

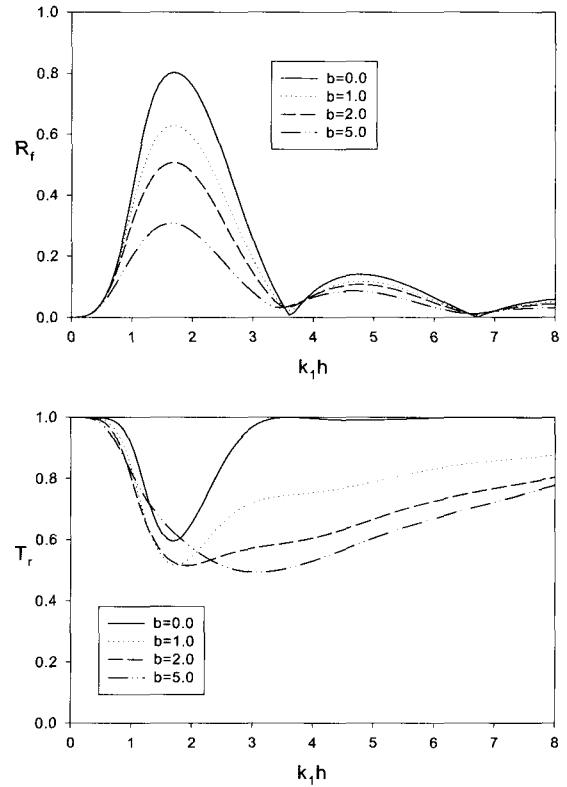


Fig. 3 Reflection coefficient and transmission coefficient of a submerged horizontal impermeable membrane as function of wavenumber $k_1 h$ for $d/h = 0.2$, $a/h = 0.5$

Fig. 4 shows transmission coefficients against dimensionless wave number for $b=2.0$ and various membrane tensions (non-dimensional tension=0.05, 0.1, 0.2, ∞). In the following, the membrane mass per unit length is 1 kg/m. The transmission coefficient increases as the tension decreases.

In Fig. 5 and 6, the reflection and transmission coefficients for $b=2.0$ and non-dimensional tension=0.1 are plotted for various submergence depths (0.1, 0.2, 0.3) and membrane lengths (0.4, 0.5, 0.6). A shallower submergence depth makes the reflection coefficient decrease.

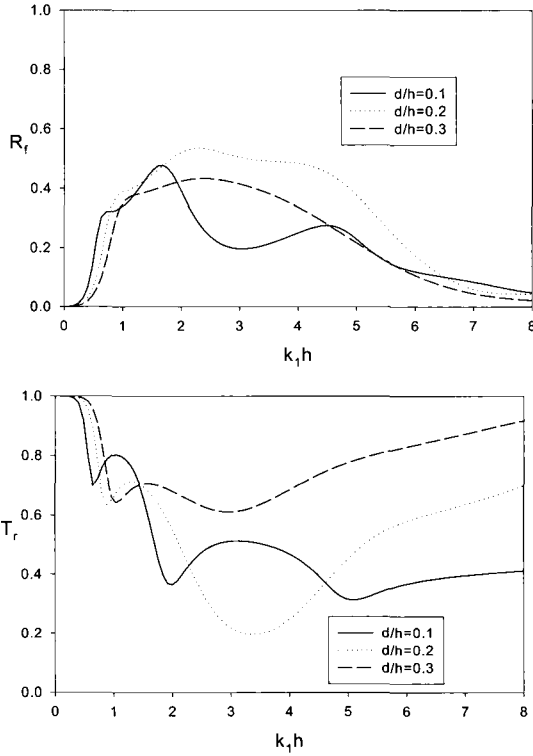


Fig. 5 Reflection coefficient and transmission coefficient of a submerged horizontal porous membrane as function of submerged depth d/h and wavenumber k_1h for $a/h=0.5$, $T/\rho gh^2=0.1$ and $b=2.0$

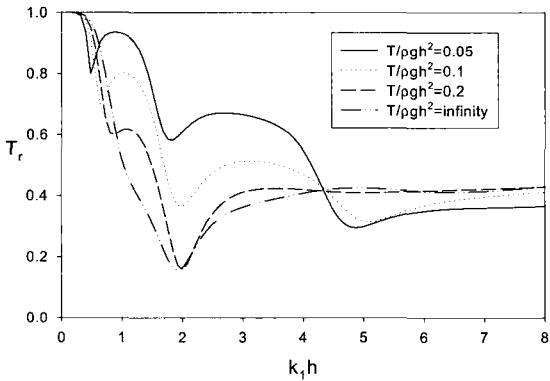


Fig. 4 Transmission coefficient of a submerged horizontal porous membrane as function of non-dimensional tension $T/\rho gh^2$ and wavenumber k_1h for $d/h=0.1$, $a/h=0.5$ and $b=2.0$

A transmission coefficient with $d/h=0.2$ shows the lower value in the region of $2.2 < k_1h < 4.7$, but transmission coefficient with $d/h=0.1$ has minimum values in the region of $k_1h > 4.7$. It is expected that a longer porous membrane reduces more wave energy, due to the viscous dissipation. The reflection coefficient follows the expected trend, but the transmission coefficient shows the contrary pattern. It is caused by the waves-induced membrane motion. We next consider the effects of membrane porosity on the wave blocking performance. In the case of porous membranes, there exists energy dissipation through pores due to fluid viscosity; thus, the energy conservation is not satisfied. Fig. 7a,b shows the reflection and transmission coefficients of a submerged membrane ($d=0.2h$) porous membrane for various b values. Wave reflection is more influenced by membrane porosity. When $k_1h > 4.5$, wave transmission decreases as b increases, while for $2.5 < k_1h < 4.5$ the transmission coefficient increases with b . The effects of membrane porosity can be positive or negative, depending on wave conditions and the given design parameters. In other words, the overall efficiency can be worse at certain wave conditions when using a porous membrane.

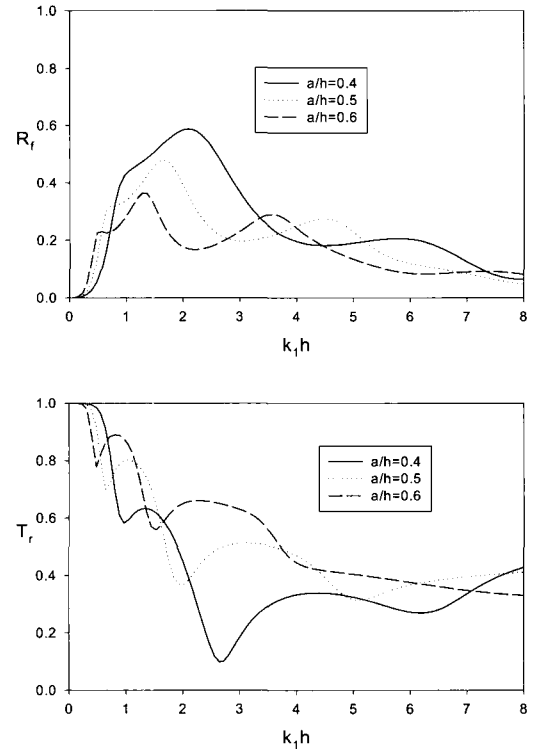


Fig. 6 Reflection coefficient and Transmission coefficient of a submerged horizontal porous membrane as function of length of membrane a/h and wavenumber k_1h for $d/h=0.1$, $T/\rho gh^2=0.1$ and $b=2.0$

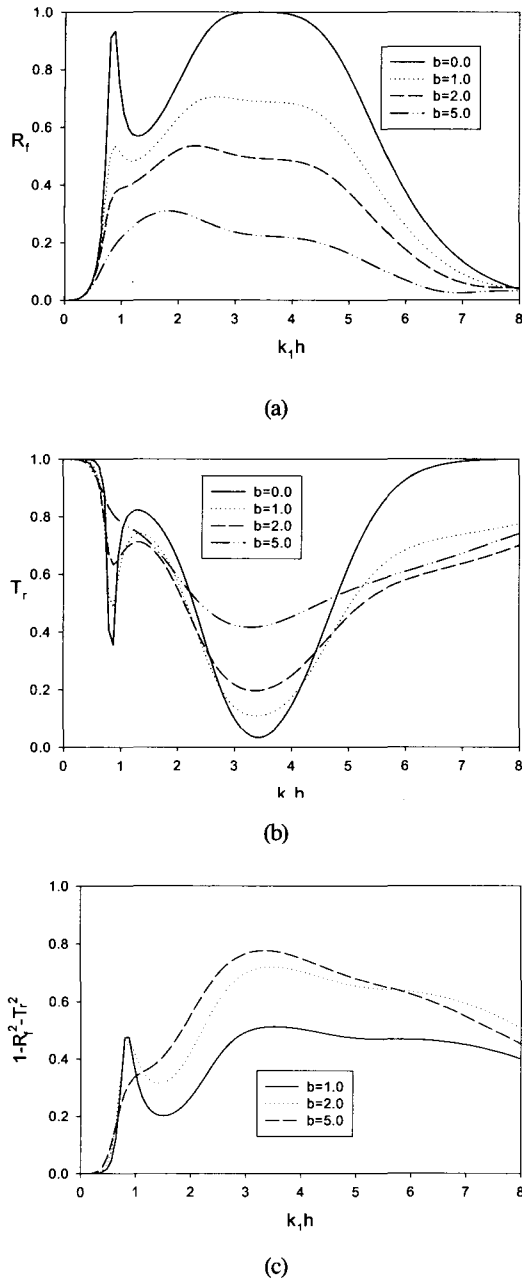


Fig. 7 Reflection coefficient, transmission coefficient and energy loss coefficient of a submerged horizontal porous membrane as function of wavenumber kh for $d/h=0.2$, $a/h=0.5$, $T/\rho gh^2=0.1$

In the case of zero porosity (or an impermeable membrane), the energy relation $R_r^2 + T_r^2 = 1$ is satisfied, while for porous cases, there exists energy dissipation, as can be seen in Fig. 7c. The energy-loss coefficient increases with b within entire frequencies range.

5. Conclusions

The interaction of monochromatic incident waves with a horizontal porous flexible membrane was investigated in the context of two-dimensional linear hydro-elastic theory. The performance of submerged porous horizontal membrane wave barriers was tested with various membrane tensions, lengths, and submergence depths. Since the horizontal membrane does not directly block incoming waves, the transmitted and motion-induced waves need to be properly cancelled to be an effective wave barrier.

On the other hand, the membrane porosity significantly increased energy dissipation by fluid viscosity, and thus reduced transmitted waves. It is seen that an optimal combination of design parameters exists for given water depths and wave characteristics and it can be determined from a parametric study.

References

- Aoki, S., Liu, H., and Sawaragi, T. (1994). "Wave transformation and wave forces on submerged vertical membrane", Proc. Intl. Symp. Waves - Physical and Numerical Modeling, Vancouver, pp 1287-1296
- Chwang, A.T. and Wu, J., (1994). "Wave scattering by submerged porous disk", J. Engrg. Mech., Vol 120, pp 2575-2587.
- Cho, I.H. and Kim, M.H. (2000). "Interactions of a horizontal porous flexible membrane with waves", J. of Waterway, Port, Coastal and Ocean Eng. ASCE, Vol 125, pp 245-253.
- Cho, I.H. and Kim, M.H. (1998). "Interactions of a horizontal flexible membrane with oblique waves", J. of Fluid Mech., Vol 356, pp 139-161.
- Cho, I.H., Kee, S.T. and Kim, M.H. (1997). "The performance of flexible-membrane wave barriers in oblique waves", J. of Applied Ocean Research, Vol 19, pp 171-182.
- Isaacson, M. and Yang, G. (1998). "Wave interactions with vertical slotted barrier", J. of Waterway, Port, Coastal and Ocean Eng. ASCE, Vol 124, pp 118-125.
- Kim, M.H. and Kee, S.T. (1996). "Flexible membrane wave barrier. Part 1. Analytic and numerical solutions", J. of Waterway, Port, Coastal and Ocean Eng. ASCE, Vol 122, pp 46-53.

- Newman, J.N. (1994). "Wave effects on deformable bodies", J. of Applied Ocean Research, Vol 16, pp 47-59.
- Thompson, G.O., Sollitt, C.K., McDougal, W.G. and Bender W.R. (1992). "Flexible membrane wave barrier", ASCE Conf. Ocean V, College Station, pp 129-148.
- Wu, J., Wan, Z. and Fang, Y. (1998). "Wave reflection by a vertical wall with a horizontal submerged porous plate", J. of Ocean Eng., Vol 25, pp 767-779.
- Yu, X. and Chwang, A.T. (1994). "Water waves above submerged porous plate", J. of Eng. Mech., Vol 120, pp 1270-1281.
-
- 2002년 8월 6일 원고 접수
2002년 12월 27일 최종 수정본 채택